Available online at www.sciencedirect.com
SCIENCE DIRECT
Trans. Nonferrous Met. Soc. China 16(2006) 828−832
Transactions of Nonferrous Metals Society of China
www.csu.edu.cn/ysxb/

Synthesis and room temperature ionic conductivity of nano-LaF_3 bulk material

WU Da-xiong(吴大雄), WU Xi-jun(吴希俊), LÜ Yan-fei(吕燕飞), WANG Hui(王 晖)

Institute of Material Physics and Microstructure, College of Materials and Chemical Engineering, Zhejiang University, Hangzhou 310027, China

Received 26 September 2005; accepted 18 April 2006

Abstract: The ionic conductivity (at room temperature) of nano-LaF_3 bulk material and a new discovered phenomenon of increasing ionic conductivity caused by grain boundary relaxation activated by AC (alternating current) shocking were reported. Nano-crystalline powder of LaF_3 with average grain size of 16.7 nm was synthesized with a method of direct precipitation from aqueous solution. Particle size and shape of LaF_3 nano-crystalline powder were analyzed by XRD and TEM. Nano-LaF_3 bulk material was prepared by compacting the powder to 1 GPa at room temperature and vacuum of 10^{-4} Pa. The ionic conductivity of nano-LaF_3 bulk material was studied with complex impedance spectra at room temperature. The ionic conductivity of nano-LaF_3 bulk material (10^{-5} S/cm) at room temperature is significantly increased compared with that of single crystal LaF_3 (10^{-6} S/cm). A special phenomenon is observed for the first time that the ionic conductivity increases gradually with AC scanning times.

Key words: nano-LaF_3; bulk material; nano-crystalline; ionic conductivity; impedance spectra

1 Introduction

Fluorides have been widely applied in many fields. They are used as components of various sensors, batteries and actuators due to their excellent electrolytes[1], as important components of toothpaste to prevent the decay of teeth, as additive of wear and crack resistant materials[2], as additive of welding materials[3] and so on.

Fluoride ion is one of the smallest anion with high mobility, thus fluorides exhibit high ionic conductivity at solid state. With the development of nano-technology, it is an effective method to increase the ionic conductivity of fluorides by fabricating the corresponding nano-crystalline bulk materials. In 1993, WU et al[4] synthesized CaF_2 nano-crystalline with average grain size of 16 nm. In a temperature range of 300−530 ℃, the ionic conductivity of nanoscale CaF_2 was 1−2 orders of magnitudes higher than that of coarse grain polycrystalline CaF_2 and CaF_2 single crystal. Later in 1995, HEITJANS reported the similar results[5]. Subsequently, WU and his group synthesized nanophase PdF_2 in the same way and the ionic conductivity was studied[6]. The results indicated that the ionic conductivity of nanophase PdF_2 was about 1 order of magnitude higher than that of coarse crystalline PdF_2.

Among all traditional coarse grain fluorides, rare earth fluorides with tysonite structure show highest ionic conductivity[7]. LaF_3 is an excellent F^- ionic conductor among other rare earth fluorides. LaF_3 based chemical sensors have been applied for sensing the fluorine, oxygen and carbon monoxide because of its high chemical stability and ionic conductivity. The ionic conductivity of LaF_3 single crystal is about 10^{-6} S/cm at room temperature[8]. Many techniques have been developed to synthesize nano-crystalline LaF_3. Recently, LaF_3 thin films with particle size ranging from 50 to 90 nm was prepared by vacuum evaporation and conductivity was studied[9]. LaF_3 superfine powder with particle size ranging from 100 to 200 nm was also synthesized with microwave heating method and compacted into a slice and then conductivity was studied [10]. The results indicated that the grain refining of LaF_3 could increase its ionic conductivity. Other methods such as microemulsion[11] and hydrothermal means[12] were applied to synthesize nano-crystalline LaF_3 powder. In this paper, we synthesized nano-crystalline LaF_3 powder with the method of direct precipitation from aqueous solution, which is simple, effective and suitable for scale

Foundation item: Project(59872031) supported by the National Natural Science Foundation of China
Corresponding author: WU Xi-jun; Tel: +86-571-87951810; E-mail: nanolab@zju.edu.cn

production. The powder was then pressed into bulk material under high pressure and high vacuum and ionic conductivity was studied.

2 Experimental

The following chemical reactions is involved in the process of LaF_3 formation:

$$La(NO_3)_3+3NH_4F=LaF_3\downarrow+3NH_4NO_3 \quad (1)$$

$La(NO_3)_3{\cdot}nH_2O$(AR) and NH_4F(AR) was dissolved in deionized water to prepared 0.3 mol/L $La(NO_3)_3$ and 1.0 mol/L NH_4F aqueous solution. All containers contacted fluoride containing solution are made of Teflon. The solutions were then mixed rapidly with stirring speed of 100 r/min and precipitation occurred immediately. After stirring for one minute, the resulting suspension was filtrated with millipore filter (0.22 μm). Precipitates were collected, and washed with deionized water several times and dried in vacuum (10^{-4} Pa) at 300 ℃ for 3 h. Thus the anhydrous LaF_3 nano-crystalline was obtained.

The resultant powder of anhydrous LaF_3 nano-crystalline was dispersed in absolute alcohol with supersonic vibration for 15 min. and then observed with transmission electron microscope(TEM, JEM200CX mode, operated at 160 kV) to study the particle size and shape.

The resultant powder of anhydrous LaF_3 nano-crystalline was put in a vacuum chamber and degassed for 2 h in a vacuum of 10^{-4} Pa. Then the powder was pressed and shaped with the pressure of 1 GPa in the same vacuum degree. After holding the pressure and vacuum for another 2 h, a disk specimen of nano-LaF_3 with 1.5 mm in thickness and 10 mm in diameter was formed. The XRD analysis of the nano-LaF_3 disk specimen was accomplished on a RIGAKU Rint 2200/PC X-ray diffraction spectrometer with Cu K_α radiation (λ=0.154 056 nm). Grain size of nano-LaF_3 was calculated by Scherrer's equation:

$$L=\frac{k\lambda}{\beta\cos\theta} \quad (2)$$

where k is 0.89. The physical broadening value β is the full-width half-maximum(FWHM) of characteristic peaks in XRD patterns. The instrumental broadening has been corrected according to Voigt function by using LaF_3 single crystal as criterion.

Finally gold was evaporated respectively on upper and lower bottom of the disk specimen in a plating machine. Gold plating can decrease the contact resistance on surface of specimen as small as possible. Thus conductivity will be measured more accurately. The ionic conductivity of nano-LaF_3 was determined by complex impedance analysis. Complex impedance measurement was completed on a LCR tester controlled with computer. Each scanning included 503 defined frequencies within the range from 12 Hz to 100 kHz. Each scanning lasted about 6 min. The scanning was repeated 20 times with 20 min interval in between. In a standard testing procedure, one may scan twice to get an average value of conductivity. In this work, we scanned 20 times to study the change tendency of conductivity. The measurement was performed at constant temperature of 300 K.

3 Results and discussion

3.1 TEM observation of nano-LaF_3 powder sample

Fig.1 shows the TEM image of nano-LaF_3 powder sample. Particles are mainly spherical with a size ranging from 10 to 20 nm. The inserted image shows the selected area diffraction(SAD) pattern of a 300 nm×300 nm area in Fig.1. The clear rings indicate that these particles are of crystalline phase. According to the classical nucleation theory[13], high super-saturation enhances nucleation process and more nuclei formed. Large number of nuclei results in small crystal size. The relation between super-saturation (S) and the radius (r) of stable nuclei can be expressed by Ostwald-Freundlish equation[14] as

$$r=\frac{2\sigma\bar{V}}{RT\ln S} \quad (3)$$

where

$$S=\left(\frac{K_{sp,t}}{K_{sp,0}}\right)^{\frac{1}{x+1}}-1$$

σ, V, R and T are surface tension, molar volume of precipitate, gas constant and absolute temperature respectively. $K_{sp,0}$ is the solubility product constant of LaF_3, and $K_{sp,0}$ is the real solubility product of LaF_3 in the reacting system. As the $K_{sp,0}$ value of LaF_3 is very low (7.0×10^{-17}), super-saturation (S) of the reacting system is very high, thus results in ultra-fine stable nuclei.

3.2 XRD analysis of nano-LaF_3 bulk material

Fig.2 shows XRD patterns of nano-LaF_3 bulk material. All peak positions are identical with that of LaF_3 (tysonite structure) in the JCPDS Card (32-0483). No other phase is found. The average grain size obtained from the broadening of (111) and (223) diffractions by Voigt function and Scherrer equation is 16.7 nm. The grain size calculated from XRD patterns is consistent with the result of TEM observation, indicating that grain

growth has not occurred during the formation of nano-LaF_3 bulk material. To avoid the grain growth, we prepared the bulk material of nano-LaF_3 at room temperature with high pressure (1 GPa) and high vacuum (10^{-4} Pa) that guarantee high density and clean interface between grains. The relative densities of resultant specimen measured with Archimedes method is 92.3%.

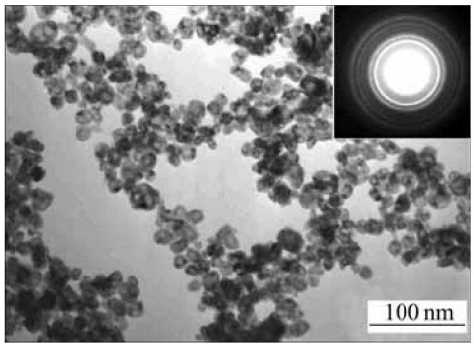

Fig.1 TEM image of nano-crystalline LaF_3 sample and corresponding SAD pattern

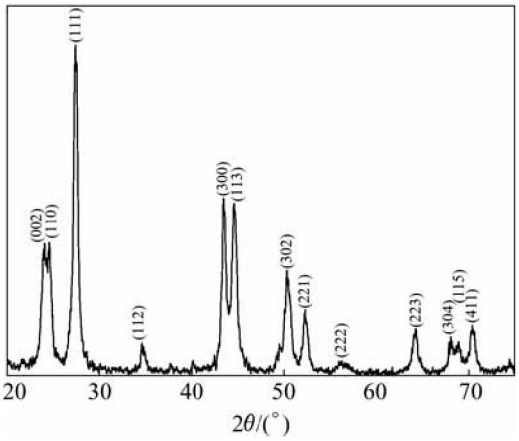

Fig.2 X-ray diffraction pattern of nano-crystalline LaF_3

3.3 Ionic conductivity of nano-LaF_3 bulk material

Fig.3 shows the typical complex impedance plots of nano-LaF_3 bulk material. Curves A, B, C, D, E, F and G represent the complex impedance of 1st, 5th, 7th, 11th, 13th, 15th and 20th scanning respectively. The equivalent circuit model is also inserted on the upper right of Fig.3. In the equivalent circuit model, resistance of grain boundary (R_{gb}) is connected in parallel with the capacitance of grain boundary (C_{gb}). The parallel circuit of R_{gb} and C_{gb} is then connected in series with the bulk resistance of grain (R_b) at one end. At the other end, the parallel circuit of R_{gb} and C_{gb} is connected in series with another parallel circuit of R_{CT} and C_{dl}. C_{dl} refers to the double-layer capacitance of electrode interface. R_{CT} refers to the transition resistance of electrode interface. The parallel circuit of R_{gb} and C_{gb} gives rise to the first arc in Fig.3, while the parallel circuit of R_{CT} and C_{dl} gives rise to the second arc. If the AC frequency of scanning is high enough, the first arc will extend to the high frequency end (to the left) and shape a semicircle as can be seen in Fig.5. The semicircle will then have two crossover points with the real axis. The crossover point at the left side represents the resistance of grain boundary (R_b). The diameter of the depressed semicircle represents the resistance of grain boundary (R_{gb}). The crossover point at the right side represents (R_b+R_{gb}), which is the real resistance applied to calculate the ionic conductivity of nano-LaF_3 bulk material. The ionic conductivity of the specimen can be then calculated by

$$Q = \frac{1}{R_b + R_{gb}} \cdot \frac{1}{S} \tag{4}$$

where L and S are the thickness and area of the specimen, respectively.

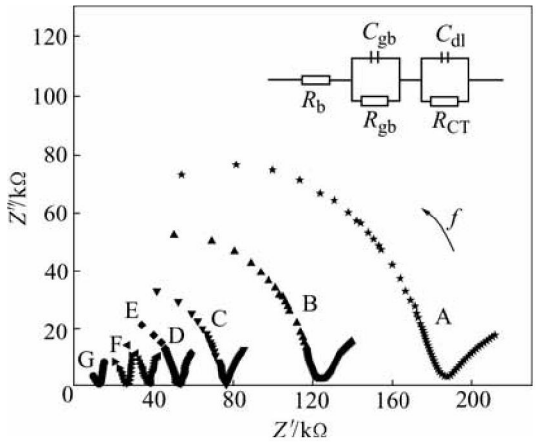

Fig.3 Complex impedance plots and equivalent circuit representation of nano-crystalline LaF_3 sample

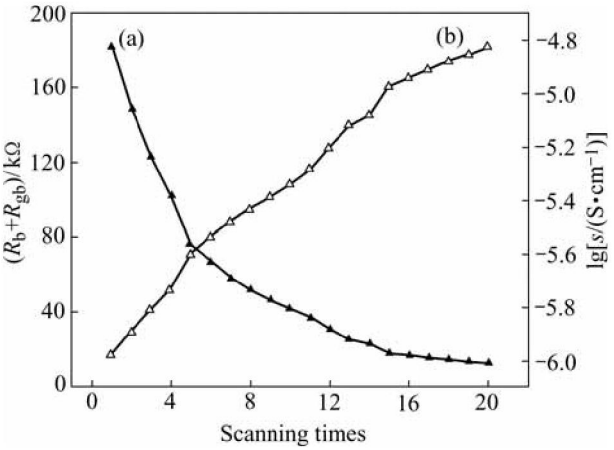

Fig.4 Resistance (a) and conductivity (b) of nano-crystalline LaF_3 vs scanning times

Curve A in Fig.3 shows the complex impedance plots of the first scanning. From curve A we know that (R_b+R_{gb}) is about 180 kΩ and the left arc is much longer

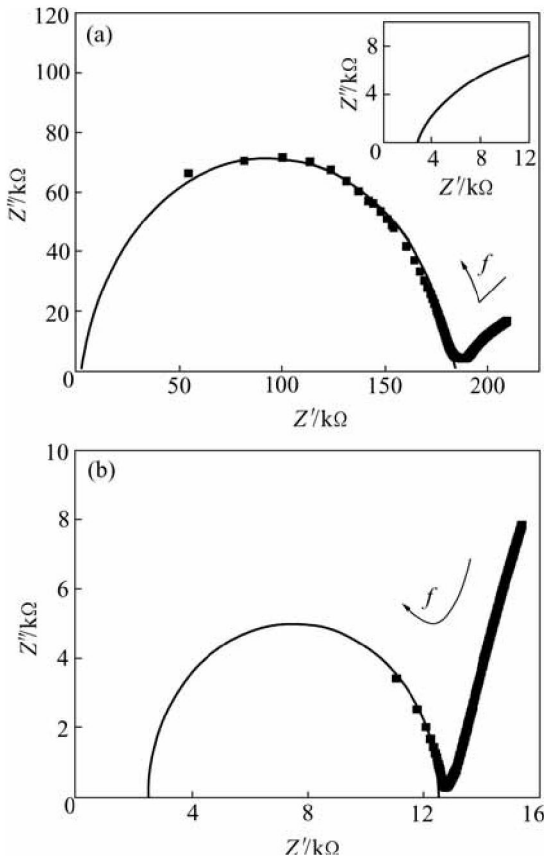

Fig.5 Complex impedance plots of first scanning(a) and 20th scanning(b)

than the right one indicating that more plots are located on the left arc. The curve contains 503 plots totally, the plots of low frequency located on the right end of the curve and those of high frequency located on the left. Curve B is the complex impedance plots of the fifth scanning. Resistance (R_b+R_{gb}) derivated from curve B is about 120 kΩ, which decreases significantly in comparison with that of the first scanning. From curve A to curve G, the crossover point representing real resistance (R_b+R_{gb}) moves to the left sequentially. In other words, the resistance of nano-LaF_3 bulk material decreases gradually from the first scanning to the 20th scanning. The tendency can also be illustrated Fig.4. Curve (a) in Fig.4 shows the decreasing tendency of the resistance (R_b+R_{gb}) with increasing scanning times. The resistance is decreased by more than 10 times after 20 scanning, which leads to an equilibrium value of about 12.5 kΩ at last. Curve (b) in Fig.4 shows the increasing tendency of the ionic conductivity, which is increased more than one order of magnitude after 20 scanning. The final value of ionic conductivity obtained from the 20th scanning is 1.5×10^{-5} S/cm which is also about one magnitude higher than that of the LaF_3 single crystal (10^{-6} S/cm).

The decrease of resistance (or increase of conductivity) of nano-LaF_3 specimen against increasing scanning times is quite similar to the decrease of resistance of fluorides against increasing temperature. The similarity also lies in the gradual change of the complex impedance plots. For a normal testing of complex impedance of fluorides, as testing temperature increases, the left arc of the complex impedance plots becomes shorter, the diameter of the depressed semicircle decreases, and the crossover point representing real resistance (R_b+R_{gb}) moves to the left. All these happened in Fig.3 from curve A to curve G. It seems that the AC scanning acts as a driving force like high temperature, which could bring rise to some kinds of change to the nano-LaF_3 specimen that favors the increase of ionic conductivity. According to the previous research[15], fluoride anions occupy different positions of the sub-lattice proportionally in LaF_3 crystal. The mobility of the fluoride anions varies with the positions that they occupy. At low temperature, most fluoride anions are difficult to move, the conductivity is contributed from small amount of highly mobile fluoride anions, and thus the conductivity is quite low. As the temperature increases, more and more fluoride anions turn to occupy the positions with high mobility in the sub-lattice, which results in relatively higher conductivity. When the temperature increase up to 500 ℃, almost all fluoride anions participate in the process of conduction.

Fig.5 shows the complex impedance plots of the first scanning and the 20th scanning (the thin lines are the fitting semicircles). From the first scanning to the 20th scanning, just like the phenomenon in heating process, real resistance (R_b+R_{gb}) of nano-LaF_3 specimen decreases from about 180 kΩ to 12.5 kΩ. Unlike the heating process, the bulk resistance of grain (R_b) basically remains constant in all scanning (the left end of fitting semicircle in Fig.5). The resistance of grain boundary (R_{gb}, diameter of the fitting semicircle in Fig.5) decreases from about 177 kΩ to 10 kΩ. But the bulk resistance of grain (R_b) is nearly 3.0 kΩ in the first scanning and about 2.5 kΩ in the 20th scanning, which is the typical value of R_b in all scanning. Such special situation leads to a theoretic hypothesis to explain the increasing conductivity of nano-LaF_3 with AC scanning. As we know, in heating process, R_b and R_{gb} decrease together because increasing temperature can activate all fluoride anions of the crystal. It seems that the AC scanning affects only those fluoride anions located at grain boundary, which is of very large proportion in LaF_3 nano-crystalline. Unlike the regular lattice inside the grain body, the grain boundary of LaF_3 nano-crystalline exists in a metastable state. The array of atoms in the grain boundary is quite irregular and the restriction of atoms is relatively weak, thus the positions of fluoride

anions are adjustable. A relatively weak activation as the alternant shock of AC scanning can provide enough driving force for the reorganization of fluoride anions. As a reaction to the alternant shock of AC scanning, many fluoride anions turn to occupy the positions in favour of conduction, so that the resistance of grain boundary (R_{gb}) decreases accordingly. As the AC scanning repeated, more and more fluoride anions turn to occupy the positions in favour of conduction results in continuous decrease of the resistance of grain boundary (R_{gb}). Eventually, after 20 scanning, the reorganization of fluoride anions reaches an equilibrium state and the increase process of ionic conductivity ceases. Essentially, the reorganization process of fluoride anions activated by AC scanning is a kind of relaxation of nano-LaF_3 bulk material and the increase scale of ionic conductivity is therefore much smaller than that of heating process.

4 Conclusions

1) Nno-LaF_3 bulk material with average grain size of 16.7 nm was prepared at room temperature with high pressure (1GPa) and high vacuum (10^{-4}Pa). Nano-crystalline powder of LaF_3 was synthesized with a method of direct precipitation from aqueous solution.

2) Ionic conductivity of nano-LaF_3 bulk material is 1.5×10^{-5} S/cm at room temperature，which is about one order of magnitude higher than that of LaF_3 single crystal (10^{-6} S/cm).

3) Repeating AC scanning results in continuous decrease of grain boundary resistance (R_{gb}) of nano-LaF_3 bulk material. It is a hypothesis that alternant shock of AC scanning activates the reorganization process of fluoride anions at grain boundary, thus increases the ionic conductivity of grain boundary.

References

[1] JEFFREY W. Fergus [J]. Sensors and Actuators B, 1997, 42: 119−130.

[2] WANG Xin-hong, SONG Si-li, ZOU Zeng-da, et al. Development of new type of wear and crack resistant hardfacing electrode [J]. Trans Nonferrous Met Soc China, 2004, 14(4): 660−664.

[3] LIU Feng-yao, YANG Chun-li, LIN San-bao, et al. Effect of weld microstructure on weld properties in A-TIG welding of titanium alloy [J]. Trans Nonferrous Met Soc China, 2003, 13(4): 876−880.

[4] WU X J, SU F, QIN X Y. Synthesis and ionic conductivity of nanophase $Ca_{1-x}La_xF_{2+x}$ [J]. Mater Res Soc Symp Proc, 1993, 286: 27−32.

[5] PUIN W, RODEWALLD S, RAMLAU R, et al. Local and overall ionic conductivity in nanocrystalline CaF_2 [J]. Solid State Ionics, 2000, 131: 159−164.

[6] LIU Jin-fang, WU Xi-jun, XU Guo-liang, et al. preparation, phase constitution and ionic conductivity of nanophase PbF_2 [J]. Journal of Inorganic Materials, 2000, 15(3): 447−450. (in Chinese)

[7] TRNOVCOVA V, GARASHINA L S, et al. Structural aspects of fast ionic conductivity of rare earth fluorides [J]. Solid State Ionics, 2003, 157: 195−201.

[8] SCHOONMAN J, OVERSLUIZEN G, WAPENAAR K E D. Solid electrolyte properties of LaF_3 [J]. Solid State Ionics, 1980, 1: 211−221.

[9] VIJAYAKUMAR M, SELVASEKARAPANDIAN S, GNANASEKARAN T, SHINOBU F, SHINNOSUKE K. Structural and impedance studies on LaF_3 thin films prepared by vacuum evaporation [J]. Journal of Fluorine Chemistry, 2004, 125(7): 1119−1125.

[10] WU Yu-feng, TIAN Yan-wen, HAN Yuan-shan, et al. Synthesis of LaF_3 superfine powder by microwave heating method [J]. Trans Nonferrous Met Soc China, 2004, 14(4): 378−341.

[11] ZHOU Jing-fang, WU Zhi-shen, ZHANG Zhi-jun, LIU Wei-min, DANG Hong-xin. Study on an antiwear and extreme pressure additive of surface coated LaF_3 nanoparticles in liquid paraffin [J]. Wear, 2001, 249: 333−337.

[12] WANG Xun, ZHUANG Jing, PENG Qing, LI Ya-dong. A general strategy for nanocrystal synthesis [J]. Nature, 2005, 437: 121−124.

[13] MULLIN J W. Crystallization [M]. Boston: Butterworth−Heinemann, 1993.

[14] ANDERSON M A, RUBIN A J. Adsorption of Inorganics at Solid-Liquid Interfaces, 1981. 145−147.

[15] HOFF C, WIEMHIJFER H D, GLUMOVB O, MURIN I V. Orientation dependence of the ionic conductivity in single crystals of lanthanum and cerium [J]. Solid State Ionics, 1997, 101: 445.

(Edited by LONG Huai-zhong)